Polymer Chemistry

Accepted Manuscript

ROYAL SOCIETY OF CHEMISTRY

www.rsc.org/polymers

Journal Name

ARTICLE

Asymmetrical Vesicles: Convenient In Situ RAFT Synthesis and Controllable Structure Determination

Received 00th January 20xx,
Accepted 00th January 20xx

DOI: 10.1039/x0xx00000x

www.rsc.org/

Zefeng Song, Xin He, Chengqiang Gao, Habib Khan, Pengfei Shi, and Wangqing Zhang*

Asymmetrical vesicles constructed with two diblock copolymers of poly(ethylene glycol)-*b*-polystyrene (PEG-*b*-PS) and poly(4-vinylpyridine)-*b*-polystyrene (P4VP-*b*-PS) were prepared through the *in situ* synthesis strategy of the two macro-RAFT agents co-mediated dispersion polymerization. The structure of the PEG-*b*-PS/P4VP-*b*-PS asymmetrical vesicles was found to be dependent on the polymerization degree (DP) of the poly(ethylene glycol) (PEG) and poly(4-vinylpyridine) (P4VP) blocks. At the cases of the DP of the P4VP block being smaller, slightly larger, and much larger than the DP of the PEG block, the P4VP chains located at the inner sides of the vesicle wall, located at both the outer and inner sides of the vesicle wall, and located at the outer side of the vesicle wall, respectively. The proposed two macro-RAFT agents co-mediated dispersion polymerization affords great convenience in synthesis of asymmetrical vesicles with well-defined structure, and it is also very helpful to understand the correlation between the block copolymer composition and the structure of asymmetrical vesicles.

1 Introduction

Block copolymer vesicles, which have enclosed bilayer structure with the solvophobic block forming the middle-layer and the solvophilic block locating at both the inner and outer sides of the solvophobic middle-layer, have attracted increasing interest in recent years, since these block copolymer vesicles have numerous applications such as tunable delivery vehicles, for the templating of biomineralization, as nanoreactors, and as scaffolds for biological conjugation.[1] Generally, two types of block copolymer vesicles as shown in Scheme 1 have been classified. The first are those of symmetrical vesicles constructed with AB diblock copolymer or ABA triblock copolymer.[2-15] Note: A and C represent the solvophilic blocks, and B represents the solvophobic block throughout the article. These symmetrical vesicles have the character that the same solvophilic A block locating at both the inner and outer sides of the solvophobic B block middle-layer, which is called the vesicle wall in the present study. The second vesicles of ABC or CBA triblock terpolymer have asymmetrical structure as shown in Scheme 1, in which the first solvophilic A block locates at one side of the vesicle wall and the third solvophilic C block locates at the other side of the vesicle wall or vice versa.[16-25] It is generally deemed that the solvophilic block with short chain-length or with low steric repulsion locates at the inner surface of the vesicle wall, and the long solvophilic block locates at the outer surface.[26-28] As is known, biological vesicles are highly asymmetrical, and this asymmetrical structure seems to be responsible for cell functions such as coagulation, membrane fusion, and stability.[32] The synthetic asymmetrical vesicles are deemed to have additional advantages such as high drug loading efficiency and efficient delivery and release.[31] However, compared with the numerous symmetrical vesicles of AB diblock copolymers or ABA triblock copolymers, asymmetrical vesicles of ABC triblock terpolymers with well-defined structure are rather limited,[26-30] and three possible reasons including (1) the laborious synthesis of well-defined ABC triblock terpolymer, (2) the lack of controlled preparation of asymmetrical vesicles, and (3) the difficult structure identification of the asymmetrical vesicles are ascribed. Therefore, convenient synthesis of asymmetrical block copolymer vesicles with well-defined structure is an interest in polymer science.

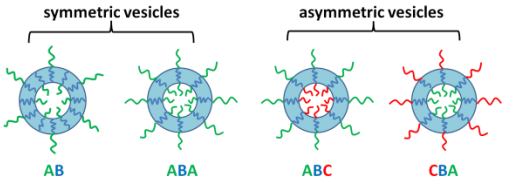

Scheme 1. Schematic structure of the symmetrical vesicles of AB and ABA block copolymers and the asymmetrical vesicles of ABC and CBA triblock terpolymers.

Self-assembly of amphiphilic block copolymer in block selective solvent is the most popular method to prepare

Key Laboratory of Functional Polymer Materials of the Ministry of Education, Collaborative Innovation Center of Chemical Science and Engineering (Tianjin), Institute of Polymer Chemistry, Nankai University, Tianjin 300071, China. E-mail: wqzhang@nankai.edu.cn

†Electronic Supplementary Information (ESI) available: See DOI: 10.1039/x0xx00000x

vesicles in these years.[33] Whereas, this strategy suffers from the inconvenience of multi procedures being included and the disadvantage of diluted block copolymer concentration usually below 1%. Besides, the size and properties of the vesicles prepared through the self-assembly strategy are highly condition-dependent and this is certainly not ideal for the general preparation and application of these materials. Recently, the *in situ* synthesis of block copolymer nano-objects by polymerization-induced self-assembly (PISA) especially through the macro-RAFT agent mediated dispersion polymerization has been demonstrated to be a valid method to prepare block copolymer nano-objects including vesicles with polymer concentration up to 30%.[34-36] Due to the high polymer concentration of the block copolymer nano-objects, the convenient one-pot *in situ* synthesis, and the tunable size and morphology of the block copolymer nano-objects just by tuning the monomer conversion during the dispersion RAFT polymerization,[37-46] the PISA strategy seems very reliable.

Recently, the strategy of the two macro-RAFT agents co-mediated dispersion polymerization has been proposed to prepare block copolymer nano-objects constructed with two diblock copolymers of AB and CB.[47-50] Compared with the general individual macro-RAFT agent mediated dispersion polymerization,[37-46] the strategy of the two macro-RAFT agents co-mediated dispersion polymerization has the character that two different macro-RAFT agents of A and C are simultaneously employed, and two diblock copolymers of AB and CB are simultaneously formed and co-assembled into mixed block copolymer nano-objects of AB/CB. By accurately tuning the character of the A and C macro-RAFT agents such as the polymerization degree (DP) and the block miscibility, the *in situ* synthesis of the mixed AB/CB block copolymer nano-objects have been achieved.[47-50] Herein, we extend the two macro-RAFT agents co-mediated dispersion polymerization to prepare asymmetrical vesicles constructed with two diblock copolymers of poly(ethylene glycol)-*b*-polystyrene (PEG-*b*-PS) and poly(4-vinylpyridine)-*b*-polystyrene (P4VP-*b*-PS). The dispersion RAFT polymerization demonstrates the successful synthesis of the asymmetrical vesicles constructed with the PEG-*b*-PS/P4VP-*b*-PS mixture, and it is also found that the structure of the PEG-*b*-PS/P4VP-*b*-PS asymmetrical vesicles is firmly dependent on the DP of the PEG and P4VP blocks.

2 Experimental

2.1 Materials

The monomers of 4-vinylpyridine (4VP, 96%, Alfa) and styrene (St, >98%, Tianjin Chemical Company) were distilled under reduced pressure prior to use. Poly(ethylene glycol) monomethyl ether (mPEG$_{45}$-OH, M_n = 2.0 kg/mol, Aldrich) was purified by azeotropic distillation with dry toluene before use. *S*-1-Dodecyl-*S*'-(a,a'-dimethyl-a''-acetic acid) trithiocarbonate (DDMAT, Figure S1) was synthesized as reported previously.[51] 2,2'-Azobis(isobutyronitrile) (AIBN, >99%, Tianjin Chemical Company, China) was recrystallized from ethanol before use. Oxalyl chloride [(COCl)$_2$, 98%, Tianjin Chemical Company, China] was freshly distilled before use. All other chemical reagents with analytical grade were purified by standard procedures or used as received. Deionized water was used.

2.2 Synthesis of poly(ethylene glycol) trithiocarbonate

The macro-RAFT agent of poly(ethylene glycol) trithiocarbonate (PEG$_{45}$-TTC, in which TTC represents the RAFT terminal of trithiocarbonate) was prepared by the esterification reaction of the hydroxy terminal in mPEG$_{45}$-OH with the carboxyl group in DDMAT as described elsewhere.[52,53] The detail synthesis is shown in Supporting Information.

2.3 Synthesis of poly(4-vinylpyridine) trithiocarbonate

Poly(4-vinylpyridine) trithiocarbonate **(**P4VP-TTC) was synthesized by solution RAFT polymerization using AIBN as initiator and DDMAT as RAFT agent. Herein, the synthesis of P4VP$_{46}$-TTC was typically introduced. Into a 50 mL Schlenk flask with a magnetic bar, DDMAT (0.6936 g, 1.9 mmol), AIBN (78.0 mg, 0.48 mmol), 4VP (10.00 g, 95 mmol), and ethanol (20.00 g) were added. The flask content was degased with nitrogen at 0 ^{0}C to remove oxygen, and then the flask was immersed into the preheated oil bath at 70 ^{0}C to initiate the RAFT polymerization. After 12 h, the polymerization was quenched by rapid cooling upon immersing the flask into ice-water, and the monomer conversion at 92% was determined by ^{1}H NMR analysis. The synthesized P4VP$_{46}$-TTC was precipitated into cold diethyl ether, collected by three precipitation/filtration cycles, and then dried at room temperature under vacuum. By tuning the molar ratio of [4VP]$_0$:[DDMAT]$_0$:[AIBN]$_0$ at 120:4:1, 200:4:1, 300:4:1 and 400:4:1, four P4VP-TTC macro-RAFT agents with different DPs, P4VP$_{29}$-TTC, P4VP$_{46}$-TTC, P4VP$_{66}$-TTC and P4VP$_{93}$-TTC, were prepared. The synthesis detail is shown in Table S1.

2.4 Synthesis of asymmetrical vesicles through two macro-RAFT agents co-mediated dispersion polymerization

The PEG$_{45}$-TTC/P4VP-TTC two macro-RAFT agents co-mediated dispersion polymerization was performed at 70 ^{0}C under [St]$_0$:[PEG$_{45}$-TTC + P4VP-TTC]$_0$:[AIBN]$_0$ = 300:1:1/3 with the weight percent of the fed St monomer plus the two macro-RAFT agents at 15%. Herein, the procedures at the case of [St]$_0$:[PEG$_{45}$-TTC]:[P4VP$_{46}$-TTC]$_0$:[AIBN]$_0$ = 300:6/7:1/7:1/3 was typically introduced. Into a Schlenk flask with a magnetic bar, PEG$_{45}$-TTC (97.0 mg, 0.041 mmol), P4VP$_{46}$-TTC (35.7 mg, 0.0069 mmol), St (1.50 g, 14.4 mmol), and AIBN (2.63 mg, 0.016 mmol) dissolved in the methanol/water mixture (80/20 by weight, 9.25 g) were added. After the flask content being degassed with nitrogen at 0 ^{0}C, the polymerization was initiated by immersing the flask into the preheated oil bath at 70 ^{0}C under gentle stirring. After a given time, the polymerization was quenched by rapid cooling upon immersing the flask into ice water. The monomer conversion was detected by UV-vis analysis at 245 nm as discussed elsewhere.[54] The resultant colloidal dispersion of the PEG-*b*-PS/P4VP-*b*-PS nano-objects was dialyzed against methanol for 3 days to remove the residual St monomer (molecular weight

cutoff: 3500 Da) to afford the methanol dispersion of the PEG-*b*-PS/P4VP-*b*-PS nano-objects. The removal of St was judged by the UV-Vis analysis of the dialysis solution at 245 nm.

2.5 Collection and separation of the PEG-b-PS/P4VP-b-PS mixture

The PEG-*b*-PS/P4VP-*b*-PS mixture was collected by directly removing the solvent in the methanol dispersion of the PEG-*b*-PS/P4VP-*b*-PS nano-objects through rotary evaporation under reduced pressure, and then dried under vacuum at room temperature.

To separate the individual diblock copolymers from the PEG-*b*-PS/P4VP-*b*-PS mixture, the mixture (0.5 g) was dispersed in the acetone/hexane mixture (6/1 by volume, 5 mL) and kept at room temperature (~20 ^{0}C) under magnetic stirring for 1 h. The mixture was separated by centrifugation (12500 r/min, 10 min), and the supernatant solution and the precipitate were collected respectively. The supernatant solution was concentrated by rotary evaporation under reduced pressure to remove the solvent completely, and then the resulted powder was dried under vacuum at room temperature to afford PEG-*b*-PS. The precipitate was re-dispersed in the 6/1 acetone/hexane mixture, and then separated by centrifugation. The supernatant solution was discarded, and the precipitate was collected and dried under vacuum at room temperature to afford P4VP-*b*-PS. The separation of P4VP-*b*-PS was monitored by ^{1}H NMR analysis, and 2 or 3 cycles of dispersion/centrifugation might be needed.

2.6 Characterization

The molecular weight and the polydispersity index (PDI, PDI = M_w/M_n) were determined by gel permeation chromatography (GPC) equipped with three SHODEX columns and a RL 2000 refractive index detector, where DMF containing LiBr (0.012 mol/L) was used as eluent at flow rate of 0.8 mL/min at 50.0 ^{0}C and the narrow-polydispersity polymethylmethacrylate (PMMA) was used as calibration standard. The ^{1}H NMR analysis was demonstrated on a Bruker Avance III 400 MHz NMR spectrometer, and for polymers dissolved in $CDCl_3$ and D_2O, the proton signal at δ = 7.26 ppm and δ = 4.79 ppm of the internal solvents were used as standard. The transmission electron microscopy (TEM) observation was performed on a Tecnai G^2 F20 electron microscope at an acceleration of 200 kV. Three different procedures for the TEM sampling were adopted. For the unstained block copolymer nano-objects, a small drop of the diluted colloidal dispersion was deposited onto a piece of copper grid, dried at room temperature, and then checked by TEM. For the block copolymer nano-objects stained by I_2 vapor, a small drop of the diluted colloidal dispersion was deposited onto a piece of copper grid, dried at room temperature, stained by I_2 vapor at 50 ^{0}C for 30 min under reduced pressure, and finally observed by TEM. For the block copolymer nano-objects jointly stained by phosphotungstic acid (PTA) and I_2 vapor, a small drop of the diluted colloidal dispersion was deposited onto a piece of copper grid, dried at room temperature, and then a drop of 1.5 wt% aqueous PTA solution was dripped onto the copper grid, dried at room temperature, and then stained by I_2 vapor at 50 ^{0}C for 30 min under reduced pressure, and finally observed by TEM.

3 Results and discussion

3.1 Synthesis of PEG-TTC and P4VP-TTC

The macro-RAFT agent of PEG_{45}-TTC was synthesized by the esterification reaction of the monohydroxyl poly(ethylene oxide) with DDMAT as discussed elsewhere.[52,53] In this synthesis, DDMAT was firstly reacted with $(COCl)_2$ to obtain the acyl chloride modified DDMAT, and then the esterification between monohydroxyl poly(ethylene oxide) and the modified DDMAT as shown in Scheme S1 was performed. Figure 1A show the ^{1}H NMR spectra of the synthesized PEG_{45}-TTC. The esterification efficiency of monohydroxyl poly(ethylene oxide) can be estimated by the area ratio of the signal at δ = 4.25 ppm (*f*) and the signal at δ = 3.26 ppm (*d*) , and it is suggested that more than 97% *m*PEG_{45}-OH is converted into PEG_{45}-TTC. According to equation S1, the molecular weight $M_{n,NMR}$ of PEG_{45}-TTC at 2.4 kg/mol can be calculated by comparing the integration areas of the signal at δ = 1.10-1.45 ppm (*b*) and the signal at δ = 3.64 ppm (*g*). It is found that the molecular weight $M_{n,NMR}$ is very close to that of the corresponding hydroxyl-terminated poly(ethylene glycol). The GPC trace of PEG_{45}-TTC is shown in Figure 2, from which the number-average molecular weight $M_{n,GPC}$ at 2.1 kg/mol and the PDI value at 1.12 are obtained.

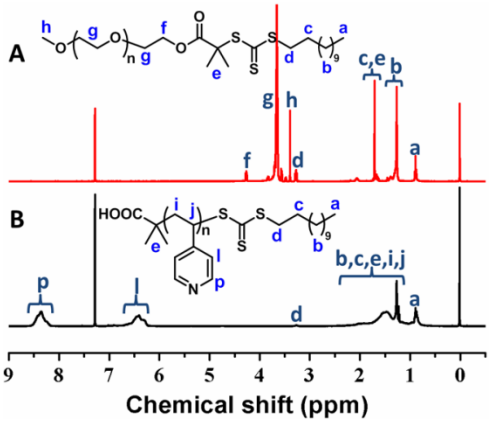

Fig. 1. The ^{1}H NMR spectra of PEG_{45}-TTC (A) and $P4VP_{46}$-TTC (B).

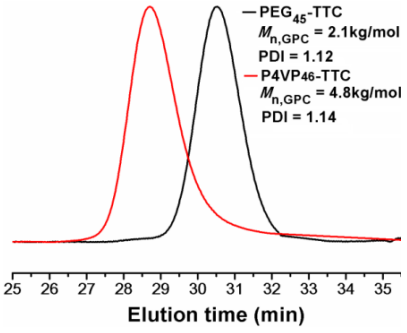

Fig. 2. The GPC traces of PEG_{45}-TTC and $P4VP_{46}$-TTC.

The P4VP-TTC macro-RAFT agent was synthesized by the solution RAFT polymerization using DDMAT as RAFT agent and AIBN as initiator. Four P4VP-TTC macro-RAFT agents with different polymerization degree, $P4VP_{29}$-TTC, $P4VP_{46}$-TTC, $P4VP_{66}$-TTC and $P4VP_{93}$-TTC, were prepared under the molar ratio of $[4VP]_0$:$[DDMAT]_0$:$[AIBN]_0$ = 120:4:1, 200:4:1, 300:4:1 and 400:4:1 with the monomer conversion at 96%, 92%, 88%, 93% (Table S1), respectively, and these four P4VP-TTC macro-RAFT agents were characterized by ^{1}H NMR analysis and GPC analysis. Figure 1B and Figure 2 show the ^{1}H NMR spectra and the GPC traces of the typical $P4VP_{46}$-TTC macro-RAFT agent, from which the molecular weight, $M_{n,NMR}$ at 5.5 kg/mol by ^{1}H NMR analysis and $M_{n,GPC}$ at 4.8 kg/mol by GPC analysis, and the molecular weight distribution index of PDI at 1.14 were obtained. Note: $M_{n,NMR}$ was calculated by comparing the integration area of the RAFT terminal at δ = 0.88 ppm (*a*) with those at δ = 8.30 ppm (*p*) corresponding to the polymer backbone following equation S2. It is found the theoretical molecular weight of $M_{n,th}$ determined by monomer conversion following equation 1,[55] and $M_{n,NMR}$ by ^{1}H NMR analysis, and $M_{n,GPC}$ by GPC analysis are close to each other, which as well as the relatively low PDI suggests the controlled synthesis of P4VP-TTC by the solution RAFT polymerization.

$$M_{n,th} = \frac{[\text{monomer}]_0 \times M_{\text{monomer}}}{[\text{RAFT}]_0} \times Conversion + M_{\text{n,macro-RAFT}} \quad (1)$$

3.2 Two macro-RAFT agents co-mediated dispersion polymerization and synthesis of asymmetrical vesicles

As discussed previously,[47-50] the PEG-TTC/P4VP-TTC two macro-RAFT agents co-mediated dispersion polymerization has a character that two different macro-RAFT agents of PEG-TTC and P4VP-TTC are simultaneously employed in the RAFT polymerization. Before the PEG-TTC/P4VP-TTC two macro-RAFT agents co-mediated dispersion polymerization being performed, the two cases of individual macro-RAFT agent mediated dispersion polymerization of styrene in the methanol/water mixture (80/20 by weight) under $[St]_0$:$[PEG_{45}$-$TTC]_0$:$[AIBN]_0$ = 300:1:1/3 or $[St]_0$:$[P4VP_{46}$-$TTC]_0$:$[AIBN]_0$ = 300:1:1/3 were checked. These two cases of individual macro-RAFT agent mediated dispersion polymerization were performed in the polymerization medium of the 80/20 methanol/water mixture under the same conditions except the difference in the macro-RAFT agent, and the 80/20 methanol/water mixture was chosen to afford the polymerization-induced self-assembly of the synthesized PEG-*b*-PS or P4VP-*b*-PS diblock copolymer as discussed elsewhere.[47-50] As shown in Figure S2, the dispersion RAFT polymerization mediated with the $P4VP_{46}$-TTC macro-RAFT agent ran faster than those mediated with the PEG_{45}-TTC macro-RAFT agent in the initial 6 h, and after that the former decelerated and the latter much accelerated, and lastly the two dispersion RAFT polymerizations approached to the similar monomer conversion of 89-92% at 14 h. This suggests that the DP of the PS block in PEG_{45}-*b*-PS is smaller than those in $P4VP_{46}$-*b*-PS in the initial polymerization stage, and the DPs of the two PS blocks become close to each other if the two dispersion RAFT polymerizations are quenched at 14 h or above 14 h. From the TEM images shown in Figure S3 and S4, it is found that the PEG_{45}-TTC macro-RAFT agent mediated dispersion polymerization affords vesicles of PEG_{45}-*b*-PS at above 25% monomer conversion in 8 h and the $P4VP_{46}$-TTC macro-RAFT agent mediated dispersion polymerization affords nanospheres of $P4VP_{46}$-*b*-PS, respectively. The ^{1}H NMR analysis (Figure S5) and GPC analysis (Figure S6) of the typical PEG_{45}-*b*-PS_{261} and $P4VP_{46}$-*b*-PS_{279} diblock copolymers prepared at 14 h confirm the good control in the polymer molecular weight and the molecular weight distribution during the dispersion RAFT polymerization, and they also indicate the similar DP of the PS block in PEG_{45}-*b*-PS_{261} and $P4VP_{46}$-*b*-PS_{279}.

With the understanding of the individual macro-RAFT agent mediated dispersion polymerization, the PEG_{45}-TTC/$P4VP_{46}$-TTC two macro-RAFT agents co-mediated dispersion polymerization under $[St]_0$:$[PEG_{45}$-$TTC]$:$[P4VP_{46}$-$TTC]_0$:$[AIBN]_0$ = 300:6/7:1/7:1/3 was performed, and the polymerization kinetics and the block copolymer morphology were checked. Clearly, the two macro-RAFT agents co-mediated dispersion polymerization was performed under the very similar conditions with the individual macro-RAFT agent mediated dispersion polymerization, *e.g.* the same molar ratio of $[monomer]_0$:$[RAFT]_0$:$[initiator]_0$ at 300:1:1/3 and the same weight percent of the fed St monomer at 15%, except that two macro-RAFT agents with the molar ratio at 6/1 were added in the polymerization medium. This similar polymerization condition afforded the convenient comparison between the individual block copolymer nano-objects of the PEG_{45}-*b*-PS vesicles and the $P4VP_{46}$-*b*-PS nanospheres with the mixed block copolymer nano-objects of PEG_{45}-*b*-PS/$P4VP_{46}$-*b*-PS, which will be discussed subsequently.

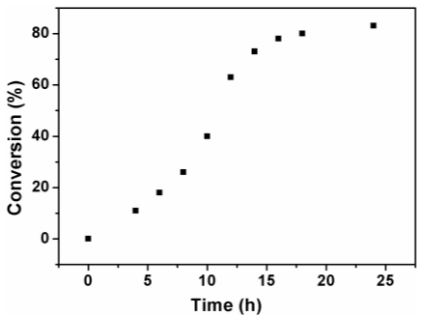

Fig. 3. The time dependent monomer conversion in the PEG_{45}-TTC/$P4VP_{46}$-TTC two macro-RAFT agents co-mediated dispersion polymerization. Polymerization conditions: St (1.50 g, 14.4 mmol), the methanol/water mixture (9.25 g, 80/20 by weight), $[St]_0$:$[PEG_{45}$-$TTC]$:$[P4VP_{46}$-$TTC]_0$:$[AIBN]_0$ = 300:6/7:1/7:1/3, 70 °C.

Figure 3 shows the polymerization kinetics of the PEG_{45}-TTC/$P4VP_{46}$-TTC two macro-RAFT agents co-mediated dispersion polymerization under $[St]_0$:$[PEG_{45}$-$TTC]$:$[P4VP_{46}$-$TTC]_0$:$[AIBN]_0$ = 300:6/7:1/7:1/3. It is found that the PEG_{45}-TTC/$P4VP_{46}$-TTC two macro-RAFT agents co-mediated dispersion polymerization runs slower than those in the presence of the $P4VP_{46}$-TTC macro-RAFT agent but similarly with those in the presence of PEG_{45}-TTC. The two macro-RAFT

agents co-mediated dispersion polymerization includes an initial 5 h homogeneous polymerization with the monomer conversion below 18% and a subsequent heterogeneous one after 5 h, which is similar with the individual macro-RAFT agent mediated dispersion polymerization reported elsewhere.[53,56,57] When the monomer conversion reaches to 83% in 24 h, the further increase in the polymerization time just leads to a very slight increase in the monomer conversion.

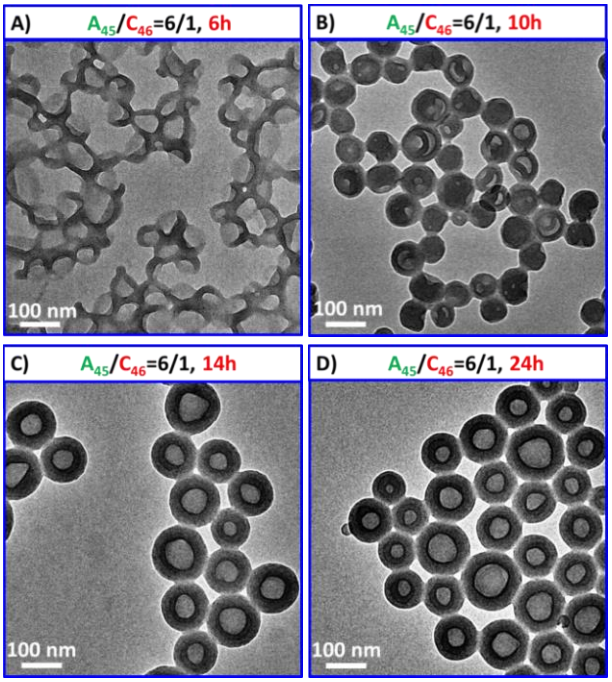

Fig. 4. The TEM images of the PEG_{45}-*b*-PS/$P4VP_{46}$-*b*-PS nano-objects prepared through the PEG_{45}-TTC/$P4VP_{46}$-TTC two macro-RAFT agents co-mediated dispersion polymerization at time of 6 h (A), 10 h (B), 14 h (C), and 24 h (D).

Figure 4 shows the TEM images of the PEG_{45}-*b*-PS/$P4VP_{46}$-*b*-PS nano-objects synthesized through the PEG_{45}-TTC/$P4VP_{46}$-TTC two macro-RAFT agents co-mediated dispersion polymerization at different polymerization times. It indicates that the morphology of the PEG_{45}-*b*-PS/$P4VP_{46}$-*b*-PS nano-objects undergoes the evolution of irregular hollow nanoparticles with the average size at ~70 nm (Figure 4A) to porous nanoparticles with average size at ~80 nm (Figure 4B), and then to vesicles with average size at ~120 nm (Figure 4C) with the increasing polymerization time. The further increase in time to 24 h makes no obvious change in the PEG_{45}-*b*-PS/$P4VP_{46}$-*b*-PS morphology (Figure 4D), and the reason is due to the slight increase in the monomer conversion as shown in Figure 3. By comparing the PEG_{45}-*b*-PS vesicles (Figure S2) and the $P4VP_{46}$-*b*-PS nanospheres (Figure S3) prepared through the individual macro-RAFT agent mediated dispersion polymerization with the present PEG_{45}-*b*-PS/$P4VP_{46}$-*b*-PS nano-objects, it is concluded that the PEG_{45}-*b*-PS/$P4VP_{46}$-*b*-PS nano-objects are composed of the two diblock copolymers of PEG_{45}-*b*-PS and $P4VP_{46}$-*b*-PS, since no nanospheres but just vesicles are formed during the two macro-RAFT agents co-mediated dispersion polymerization.

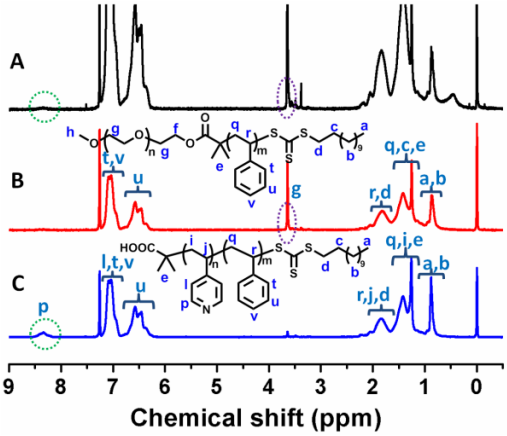

Fig. 5. The ^{1}H NMR spectra of the PEG_{45}-*b*-PS_{219}/$P4VP_{46}$-*b*-PS_{219} mixture (A) and the separated diblock copolymers of PEG_{45}-*b*-PS_{219} (B) and $P4VP_{46}$-*b*-PS_{219} (C).

To detect the exact chemical composition of the PEG_{45}-*b*-PS/$P4VP_{46}$-*b*-PS vesicles, the typical vesicles synthesized at 14 h were collected, and the PEG_{45}-*b*-PS/$P4VP_{46}$-*b*-PS mixture was separated. Since PEG_{45}-*b*-PS is somewhat soluble in the 6/1 acetone/hexane mixture, whereas $P4VP_{46}$-*b*-PS is insoluble at all, thus separation of PEG_{45}-*b*-PS and $P4VP_{46}$-*b*-PS from the PEG_{45}-*b*-PS/$P4VP_{46}$-*b*-PS mixture can be achieved through several cycles of dispersion/centrifugation. Figure 5 shows the ^{1}H NMR spectra of the PEG_{45}-*b*-PS/$P4VP_{46}$-*b*-PS mixture (Figure 5A) and the separated diblock copolymers of PEG_{45}-*b*-PS (Figure 5B) and $P4VP_{46}$-*b*-PS (Figure 5C). By comparing the signals at δ = 3.64 ppm and 8.30 ppm shown in Figure 5A, the molar ratio of PEG_{45}-*b*-PS/$P4VP_{46}$-*b*-PS in the PEG_{45}-*b*-PS/$P4VP_{46}$-*b*-PS mixture at 5.73/1 is obtained, which is very close to the molar ratio of the fed PEG_{45}-TTC/$P4VP_{46}$-TTC macro-RAFT agents, suggesting that all the macro-RAFT agents are block-extended to form the corresponding diblock copolymers. By checking the signals at δ = 3.64 ppm and 8.30 ppm, which are indicated out by green cycles, it is concluded that successful separation is made. Note: based on Figure 5C, about 7% PEG_{45}-*b*-PS is immerged in the separated $P4VP_{46}$-*b*-PS. From the ^{1}H NMR spectra of the separated diblock copolymers, the molecular weight of the diblock copolymers by ^{1}H NMR analysis, $M_{n,NMR}$ of PEG_{45}-*b*-PS at 27.1 kg/mol and $M_{n,NMR}$ of $P4VP_{46}$-*b*-PS at 27.0 kg/mol, are calculated. By assuming the DPs of the PS block in PEG_{45}-*b*-PS and $P4VP_{46}$-*b*-PS being equal to each other, the theoretical molecular weight, $M_{n,th}$ at 25.1 kg/mol corresponding to PEG_{45}-*b*-PS_{219} and $M_{n,th}$ at 27.9 kg/mol corresponding to $P4VP_{46}$-*b*-PS_{219}, is calculated following equation 1. Clearly, $M_{n,NMR}$ and $M_{n,th}$ are close to each other whether in the case of PEG_{45}-*b*-PS diblock copolymer or in the case of the $P4VP_{46}$-*b*-PS diblock copolymer. These diblock copolymers before separation and after separation are also characterized by GPC analysis. From the GPC traces shown in Figure 6, the molecular weight of the diblock copolymers by GPC analysis, $M_{n,GPC}$ at 29.4 kg/mol for PEG_{45}-*b*-PS with PDI = 1.19 and $M_{n,GPC}$ at 24.2 kg/mol for $P4VP_{46}$-*b*-PS with PDI = 1.15, are obtained. Thus, based on the ^{1}H NMR analysis and the GPC analysis of the diblock copolymers before and after separation,

two conclusions are made. First, in the PEG_{45}-*b*-PS/$P4VP_{46}$-*b*-PS vesicles, the three values of the molecular weight of the PEG_{45}-*b*-PS or $P4VP_{46}$-*b*-PS diblock copolymer, $M_{n,NMR}$, $M_{n,GPC}$ and $M_{n,th}$, are close to each other or just slightly different. Second, in the PEG_{45}-*b*-PS/$P4VP_{46}$-*b*-PS vesicles, the DP of the PS block in PEG_{45}-*b*-PS is close to that in $P4VP_{46}$-*b*-PS. In the following discussion, the PEG_{45}-*b*-PS/$P4VP_{46}$-*b*-PS vesicles are labeled $A_{45}B_n/C_{46}B_n$ vesicles, in which A, B and C represent the PEG, PS and P4VP blocks, respectively, and the DP of the PS block in the two diblock copolymers is deemed to be equal to each other and the DP value of the PS block is determined by $M_{n,th}$.

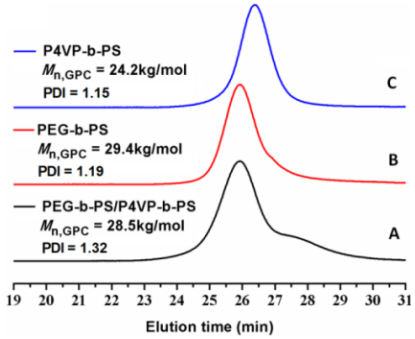

Fig. 6. The GPC traces of the PEG_{45}-*b*-PS_{219}/$P4VP_{46}$-*b*-PS_{219} mixture (A) and the separated diblock copolymers of PEG_{45}-*b*-PS_{219} (B) and $P4VP_{46}$-*b*-PS_{219} (C).

Now, we focused on the topologic structure of the $A_{45}B_{219}/C_{46}B_{219}$ vesicles, which were prepared through the PEG_{45}-TTC/$P4VP_{46}$-TTC two macro-RAFT agents co-mediated dispersion polymerization at 14 h. To detect the exact location of the P4VP chains in the $A_{45}B_{219}/C_{46}B_{219}$ vesicles, the unstained $A_{45}B_{219}/C_{46}B_{219}$ vesicles, the $A_{45}B_{219}/C_{46}B_{219}$ vesicles stained by I_2 vapor, and the $A_{45}B_{219}/C_{46}B_{219}$ vesicles stained initially by PTA and then by I_2 vapor are checked by TEM, respectively, and the TEM images are shown in Figure 7A, 7B and 7C. Note: I_2 vapor can selectively stain the P4VP phase as discussed elsewhere;[58,59] PTA, which can form salt-like complex with the amino group, is usually used to stain the amino-cotaining molecules.[61,62] Therefore, the combination use of I_2 vapor and PTA helps to clearly discern the P4VP phase in the $A_{45}B_{219}/C_{46}B_{219}$ vesicles.[47,60] By checking the TEM images shown in Figure 7A, 7B and 7C, no obvious contrast between the inner wall and the outer wall is found. Therefore, it is concluded that the $P4VP_{46}$ chains locate at the inner side of the vesicle wall but not at the outer side. Note: this will be further discussed subsequently. However, herein we cannot make a neat estimation that whether the sole $P4VP_{46}$ chains or the $P4VP_{46}/PEG_{45}$ mixed chains locate at the inner side of the vesicle wall. Based on the similar DP of the $P4VP_{46}$ and PEG_{45} blocks, the PEG_{45}-TTC/$P4VP_{46}$-TTC molar ratio at 6/1, and the ratio of the outer surface area to the inner surface area of the $A_{45}B_{219}/C_{46}B_{219}$ vesicles at ~4/1, which is approximately calculated based on the average size and the wall thickness of the $A_{45}B_{219}/C_{46}B_{219}$ vesicles followed equation S3, it is expected that the mixed $P4VP_{46}/PEG_{45}$ chains locate at the inner side and the sole PEG_{45} chains locate at the outer side of the vesicle wall in the $A_{45}B_{219}/C_{46}B_{219}$ asymmetrical vesicles as shown in Figure 7D.

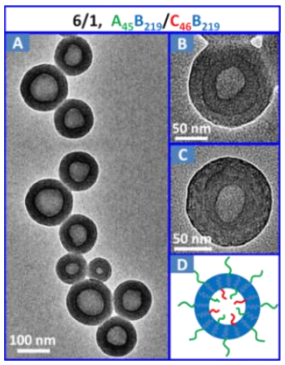

Fig. 7. The TEM images of the $A_{45}B_{219}/C_{46}B_{219}$ vesicles: unstained vesicles (A), vesicles stained by I_2 vapor (B), and vesicles stained by PTA and I_2 vapor (C), and the schematic structure of the $A_{45}B_{219}/C_{46}B_{219}$ vesicles (D).

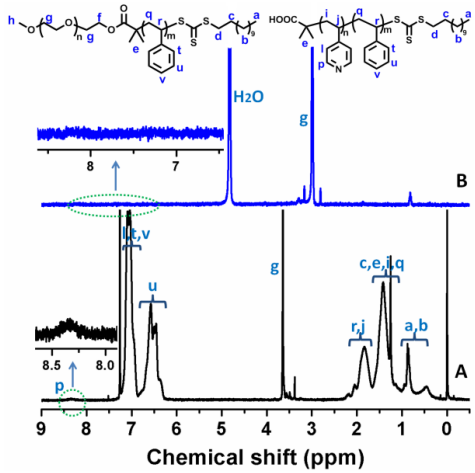

Fig. 8. The ^{1}H NMR spectra of the $A_{45}B_{219}/C_{46}B_{219}$ vesicles dispersed in acidic D_2O at pH = 1 (A) and the reference PEG_{45}-*b*-PS_{219}/$P4VP_{46}$-*b*-PS_{219} molecularly dissolved in $CDCl_3$ (B).

To further explore the exact location of the $P4VP_{46}$ chains in the $A_{45}B_{219}/C_{46}B_{219}$ asymmetrical vesicles, the $A_{45}B_{219}/C_{46}B_{219}$ vesicles dispersed in acidic D_2O at pH = 1 as well as the reference of PEG_{45}-*b*-PS_{219}/$P4VP_{46}$-*b*-PS_{219} molecularly dissolved in $CDCl_3$ were checked by ^{1}H NMR analysis. In this acidic D_2O at pH = 1, both the PEG chains and the acidified P4VP chains are soluble, and the wall-formed PS block is insoluble. As shown in Figure 8A, no signal ascribed to the acidified $P4VP_{46}$ chains but just the signal at δ = 3.02 ppm (*g*) ascribed to the PEG_{45} chains is detected (Figure 8A). Whereas, in the PEG_{45}-*b*-PS_{219}/$P4VP_{46}$-*b*-PS_{29} reference, the signals ascribed to both the PEG_{45} chains at δ = 3.64 ppm (*g*) and the $P4VP_{46}$ chains at δ = 8.30 ppm (*p*) are detected. This clearly suggests that the $P4VP_{46}$ chains in the $A_{45}B_{219}/C_{46}B_{219}$ vesicles are shielded by the insoluble PS chains and therefore are unascertainable, and therefore the conclusion that the $P4VP_{46}$ chains locate at the inner side of the vesicle wall as shown in Figure 7D is made.

3.3 Effect of the PEG_{45}-TTC/$P4VP_{46}$-TTC molar ratio on formation of asymmetrical vesicles

The PEG_{45}-TTC/$P4VP_{46}$-TTC two macro-RAFT agents co-mediated dispersion polymerization under different molar ratio of PEG_{45}-TTC/$P4VP_{46}$-TTC but keeping the constant $[St]_0$:$[PEG_{45}$-TTC + $P4VP_{46}$-TTC$]_0$:$[AIBN]_0$ = 300:1:1/3 was performed and the PEG_{45}-*b*-PS/$P4VP_{46}$-*b*-PS nano-objects were checked. It was found that the monomer conversion in 14 h in the PEG_{45}-TTC/$P4VP_{46}$-TTC two macro-RAFT agents co-mediated dispersion polymerization under different molar ratio of PEG_{45}-TTC/$P4VP_{46}$-TTC was similar (73~93%), whereas the morphology of the PEG_{45}-*b*-PS/$P4VP_{46}$-*b*-PS nano-objects was firmly dependent on the PEG_{45}-TTC/$P4VP_{46}$-TTC molar ratio. As shown in Figure 9, in the case of low $P4VP_{46}$-TTC content in the fed PEG_{45}-TTC/$P4VP_{46}$-TTC macro-RAFT agents, such as the PEG_{45}-TTC/$P4VP_{46}$-TTC molar ratio at 1/0 (Figure 9A), 6/1(Figure 9B) and 4/1 (Figure 9C), vesicles are formed; in the case of the moderate $P4VP_{46}$-TTC content, the mixture of vesicles and nanospheres are formed (Figure 9D); and in the case of high $P4VP_{46}$-TTC content, such as the PEG_{45}-TTC/$P4VP_{46}$-TTC molar ratio at 1/1 (Figure 9E) and 0/1 (Figure 9F), nanospheres are formed, respectively. Note: at the cases of PEG_{45}-TTC/$P4VP_{46}$-TTC = 1/0 and 0/1, the two cases of individual macro-RAFT agent mediated dispersion polymerization were performed. This suggests that the PEG-*b*-PS/P4VP-*b*-PS asymmetrical vesicles can only be formed at high PEG_{45}-TTC/$P4VP_{46}$-TTC molar ratio, and the PEG-*b*-PS/P4VP-*b*-PS nanospheres were formed at low PEG_{45}-TTC/$P4VP_{46}$-TTC molar ratio. This is not surprised, since the PEG_{45}-TTC macro-RAFT agent mediated dispersion polymerization tends to afford PEG_{45}-*b*-PS vesicles and the $P4VP_{46}$-TTC macro-RAFT agent mediated dispersion polymerization tends to afford $P4VP_{46}$-*b*-PS nanospheres as discussed above.

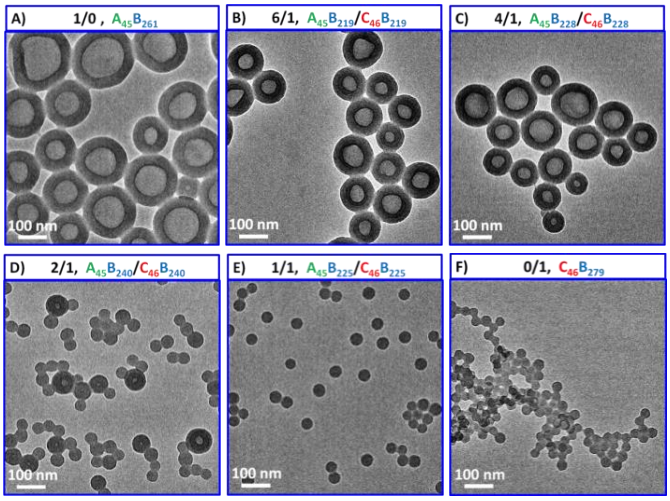

Fig. 9. The TEM images of the PEG-*b*-PS/P4VP-*b*-PS nano-objects formed through the PEG_{45}-TTC/$P4VP_{46}$-TTC two macro-RAFT agents co-mediated dispersion polymerization with the PEG_{45}-TTC/$P4VP_{46}$-TTC molar ratio at 1/0 (A), 6/1(B), 4/1 (C), 2/1 (D), 1/1 (E) and 0/1 (F).

3.4 DP dependent location of the P4VP chains in the PEG-b-PS/P4VP-b-PS asymmetrical vesicles

For asymmetrical vesicles of ABC or CBA triblock terpolymer, it is deemed that the long solvophilic block locates at the outer side and the short solvophilic block locates at the inner side of the vesicle wall.[26-28,31] Herein, to investigate how the chain-length or DP of the P4VP chains affecting their location in the PEG-*b*-PS/P4VP-*b*-PS asymmetrical vesicles, the PEG_{45}-TTC/P4VP-TTC two macro-RAFT agents co-mediated dispersion polymerization employing four different P4VP-TTC macro-RAFT agents of $P4VP_{29}$-TTC, $P4VP_{46}$-TTC, $P4VP_{66}$-TTC and $P4VP_{93}$-TTC under the same conditions such as the constant molar ratio of PEG_{45}-TTC/P4VP-TTC at 6/1 and the constant $[St]_0$:$[PEG_{45}$-TTC + P4VP-TTC$]_0$:$[AIBN]_0$ = 300:1:1/3 was performed. Note: the PEG-TTC/P4VP-TTC two macro-RAFT agents co-mediated dispersion polymerization employing different PEG-TTC macro-RAFT agents but the same $P4VP_{46}$-TTC was not checked, since nanospheres but not vesicles were formed in the longer PEG-TTC macro-RAFT agent mediated dispersion polymerization as discussed elsewhere.[53]

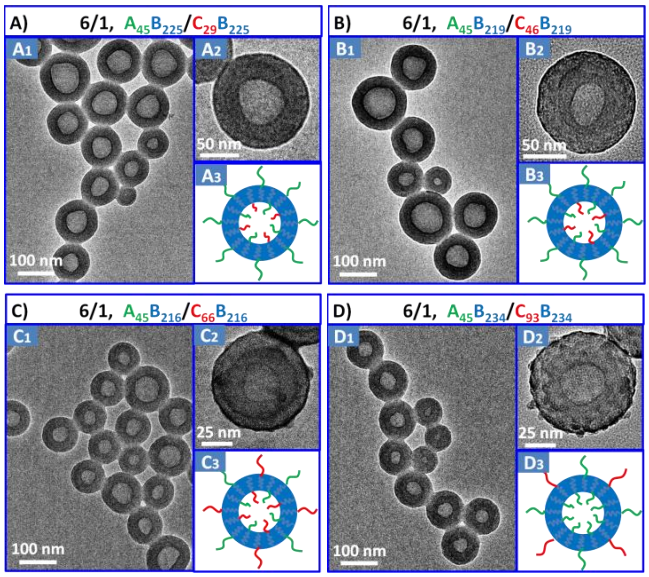

Fig. 10. The TEM images and the schematic structure of the asymmetrical vesicles of PEG_{45}-*b*-PS_{225}/$P4VP_{29}$-*b*-PS_{225} (A), PEG_{45}-*b*-PS_{219}/$P4VP_{46}$-*b*-PS_{219} (B), PEG_{45}-*b*-PS_{216}/$P4VP_{66}$-*b*-PS_{216} (C), and PEG_{45}-*b*-PS_{234}/$P4VP_{93}$-*b*-PS_{234} (D). Note: unstained vesicles (A1, B1, C1 and D1), vesicles stained by PTA and I_2 vapor (A2, B2, C2 and D2), and the schematic structure of the asymmetrical vesicles (A3, B3, C3 and D3).

After the PEG_{45}-TTC/P4VP-TTC two macro-RAFT agents co-mediated dispersion polymerization being quenched in 14 h, it was found that the very similar monomer conversion at 73-78% was achieved in the four cases of the two macro-RAFT agents co-mediated dispersion polymerization, although the DP of the P4VP-TTC macro-RAFT agent is different. The morphology of the PEG-*b*-PS/P4VP-*b*-PS nano-objects were checked (Figure 10), and the separation of the individual diblock copolymers from the PEG-*b*-PS/P4VP-*b*-PS mixture was performed, and the characterization of the separated diblock copolymers was made (Figure S7). Note: the molecular weight of PEG-*b*-PS and

P4VP-*b*-PS determined by monomer conversion is shown as inset in Figure 10. From the TEM images shown in Figure 10, formation of the PEG-*b*-PS/P4VP-*b*-PS vesicles with average size at 90-120 nm is found in the four cases of the PEG_{45}-TTC/P4VP-TTC two macro-RAFT agents co-mediated dispersion polymerization. To discern the P4VP location in the vesicles, the vesicles were further stained by PTA and I_2 vapor, and the TEM images are shown in Figures 10A2, B2, C2 and D2. By carefully checking the TEM images of the stained vesicles, the vesicles with a smooth outer-side (Figures 10A2 and B2), the vesicles with a silightly stained outer-side (Figure 10C2), and the vesicles with a highly stained outer-side (Figure 10D2) are dectected, respectively. This suggests that the location of the P4VP chains in the PEG-*b*-PS/P4VP-*b*-PS vesicles is firmly dependent on the DP of the P4VP chains, which is schematically shown in Figures 10A3, B3, C3 and D3. That is, when the DP of the P4VP chains is smaller than or equal to that of the PEG_{45} chains, the P4VP chains locate at the inner side of the vesicle wall in the PEG-*b*-PS/P4VP-*b*-PS vesicles; when the DP of the P4VP chains is slightly larger than that of the PEG_{45} chains (66 *vs* 45), the P4VP chains begin to locate at the outer side of the vesicle wall; when the DP of the P4VP chains is much larger than that of the PEG_{45} chains (93 *vs* 45), the P4VP chains locate at the outer side of the vesicle wall, respectively.

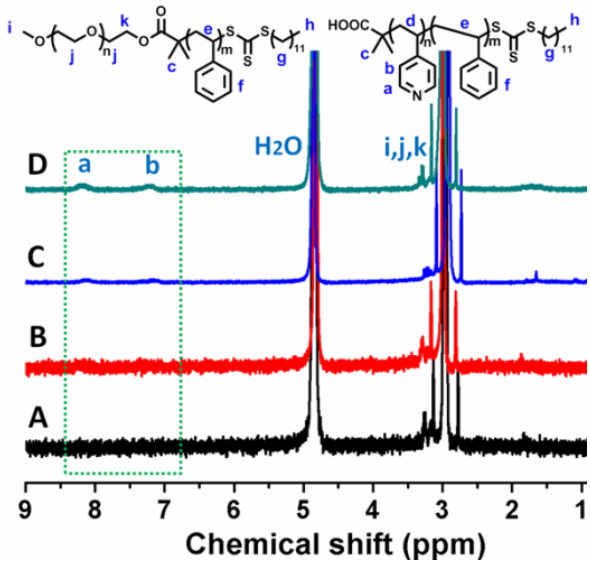

Fig. 11. The ^{1}H NMR spectra of the PEG-*b*-PS/P4VP-*b*-PS vesicles dispersed in acidic D_2O at pH =1: (A) the PEG_{45}-*b*-PS_{225}/$P4VP_{29}$-*b*-PS_{225} vesicles, (B) the PEG_{45}-*b*-PS_{219}/$P4VP_{46}$-*b*-PS_{219} vesicles, (C) the PEG_{45}-*b*-PS_{216}/$P4VP_{66}$-*b*-PS_{216} vesicles, and (D) the PEG_{45}-*b*-PS_{234}/$P4VP_{93}$-*b*-PS_{234} vesicles.

Further, from the ^{1}H NMR spectra of the PEG-*b*-PS/P4VP-*b*-PS vesicles dispersed in acidic D_2O shown in Figure 11, the difference in the four PEG-*b*-PS/P4VP-*b*-PS asymmetrical vesicles is observed. That is, in the PEG-*b*-PS/P4VP-*b*-PS vesicles including short P4VP chains (Figure 11A and 11B), the signals just ascribed to the PEG chains (*j* at δ = 3.02 ppm) are detected, and in PEG-*b*-PS/P4VP-*b*-PS vesicles including long P4VP chains (Figure 11C and 11D), the signals ascribed to both the PEG chains (*j* at δ = 3.02 ppm) and the P4VP chains (*a* at δ = 8.30 ppm and *b* at δ = 7.18 ppm as indicated by green square) were detected. This ^{1}H NMR analysis confirms the DP dependent location of the P4VP chains in the PEG-*b*-PS/P4VP-*b*-PS asymmetrical vesicles as schematically shown in Figure 10. Note: the mixed $P4VP_{93}$/PEG_{45} chains locate at the outer side of the vesicle wall in the PEG_{45}-*b*-PS_{234}/$P4VP_{93}$-*b*-PS_{234} asymmetrical vesicles as shown in Figure 10D3, and this expectation is made due to the low $P4VP_{93}$/PEG_{45} molar ratio at 1/6 and the relatively high outer surface area in the PEG_{45}-*b*-PS_{234}/$P4VP_{93}$-*b*-PS_{234} asymmetrical vesicles

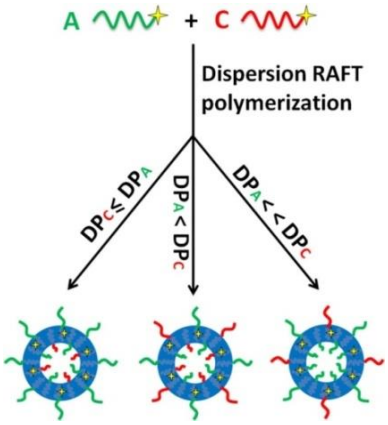

Scheme 2. Summary of the PEG-*b*-PS/P4VP-*b*-PS asymmetrical vesicles prepared through the PEG_{45}-TTC/P4VP-TTC two macro-RAFT agents co-mediated dispersion polymerization, in which A represents the PEG_{45}-TTC macro-RAFT agent and C represents the P4VP-TTC macro-RAFT agent.

Summarily, our main finding in the formation of the PEG-*b*-PS/P4VP-*b*-PS asymmetrical vesicles through the PEG_{45}-TTC/P4VP-TTC two macro-RAFT agents co-mediated dispersion polymerization is shown in Scheme 2. When the DP of the P4VP-TTC macro-RAFT agent is smaller than or equal to that of the PEG_{45}-TTC macro-RAFT agent, the P4VP chains locate at the inner sides of the vesicle wall in the PEG-*b*-PS/P4VP-*b*-PS asymmetrical vesicles; with the increasing DP of the P4VP-TTC macro-RAFT agent above that of PEG_{45}-TTC, the P4VP chains locate at both the outer and inner sides of the vesicle wall; in the case of the DP of the P4VP-TTC macro-RAFT agent much higher than that of PEG_{45}-TTC, the P4VP chains locate at the outer side of the vesicle wall, respectively.

4 Conclusions

Asymmetrical vesicles constructed with two diblock copolymers of PEG-*b*-PS/P4VP-*b*-PS were prepared through the PEG_{45}-TTC/P4VP-TTC two macro-RAFT agents co-mediated dispersion polymerization of styrene in the methanol/water mixture. During the two macro-RAFT agents co-mediated dispersion polymerization, the two diblock copolymers of PEG-*b*-PS and P4VP-*b*-PS were simultaneously formed and co-assembled into nano-objects constructed with the two diblock copolymers of PEG-*b*-PS and P4VP-*b*-PS. It was found that the

morphology of the PEG-*b*-PS/P4VP-*b*-PS nano-objects was dependent on the macro-RAFT agent molar ratio of PEG_{45}-TTC/P4VP-TTC, and the PEG-*b*-PS/P4VP-*b*-PS asymmetrical vesicles were formed at high PEG_{45}-TTC/P4VP-TTC ratio. The structure of the PEG-*b*-PS/P4VP-*b*-PS asymmetrical vesicles was found to be dependent on the DP of the PEG and P4VP blocks. At the cases of DP of the P4VP block being smaller, slightly larger and much larger than the DP of the PEG block, the P4VP chains locate at the inner sides of the vesicle wall, locate at both the outer and inner sides of the vesicle wall, and locate at the outer side of the vesicle wall, respectively. The proposed two macro-RAFT agents co-mediated dispersion polymerization afford a convenient *in situ* synthesis of asymmetrical vesicles with well-defined structure, which is believed to be very useful in the vesicle preparation and in the understanding of the vesicle structure.

Acknowledgements

The financial support by National Science Foundation of China (№ 21274066 and 21474054) and PCSIRT (IRT1257) is gratefully acknowledged.

Notes and references

1 J. Du and R. K. O'Reilly, *Soft Matter*, 2009, **5**, 3544-3561.
2 T. Azzam and A. Eisenberg, *Angew. Chem. Int. Ed.*, 2006, **45**, 7443-7447.
3 J. del Barrio, L. Oriol, C. Sánchez, J. L. Serrano, A. D. Cicco, P. Keller and M.-H. Li, *J. Am. Chem. Soc.*, 2010, **132**, 3762-3769.
4 W. Qi, P. P. Ghoroghchian, G. Li, D. A. Hammer and M. J. Therien, *Nanoscale*, 2013, **5**, 10908-10915.
5 J. Huang, C. Bonduelle, J. Thévenot, S. Lecommandoux and A. Heise, *J. Am. Chem. Soc.*, 2012, **134**, 119-122.
6 A. Feng, C. Zhan, Q. Yan, B. Liu and J. Yuan, *Chem. Commun.*, 2014, **50**, 8958-8961.
7 L. Yin, T. P. Lodge and M. A. Hillmyer, *Macromolecules*, 2012, **45**, 9460-9467.
8 Y. Liu, C. Yu, H. Jin, B. Jiang, X. Zhu, Y. Zhou, Z. Lu and D. Yan, *J. Am. Chem. Soc.*, 2013, **135**, 4765-4770.
9 M. T. Savoji, S. Strandman and X. X. Zhu, *Soft Matter*, 2014, **10**, 5886-5893.
10 H. Zhu, Q. Liu and Y. Chen, *Langmuir*, 2007, **23**, 790-794.
11 Y. Han, H. Yu, H. Du and W. Jiang, *J. Am. Chem. Soc.*, 2010, **132**, 1144-1150.
12 G. Liu, X. Wang, J. Hu, G. Zhang and S. Liu, *J. Am. Chem. Soc.*, 2014, **136**, 7492-7497.
13 E. V. Korchagina, X.-P. Qiu and F. M. Winnik, *Macromolecules*, 2013, **46**, 2341-2351.
14 N. V. Salim and Q. Guo, *J. Phys. Chem. B*, 2011, **115**, 9528-953.
15 A. E. Smith, X. Xu, S. E. Kirkland-York, D. A. Savin and C. L. McCormick, *Macromolecules*, 2010, **43**, 1210-1217.
16 C. Ott, R. Hoogenboom, S. Hoeppener, D. Wouters, J.-F. Gohy and U. S. Schubert, *Soft Matter*, 2009, **5**, 84-91.
17 J. Hu, T. Wu, G. Zhang and S. Liu, *J. Am. Chem. Soc.*, 2012, **134**, 7624-7627.
18 G. Njikang, D. Han, J. Wang and G. Liu, *Macromolecules*, 2008, **41**, 9727-9735.
19 C. Luo, Y. Liu and Z. Li, *Soft Matter*, 2012, **8**, 2618-2626.
20 Q. Yan and Y. Zhao, *J. Am. Chem. Soc.*, 2013, **135**, 16300-16303.
21 K. Kempe, R. Hoogenboom, S. Hoeppener, C.-A. Fustin, J.-F. Gohy and U. S. Schubert, *Chem. Commun.*, 2010, **46**, 6455-6457.
22 R. Zheng and G. Liu, *Macromolecules*, 2007, **40**, 5116-5121.
23 E. Betthausen, C. Hanske, M. Müller, A. Fery, F. H. Schacher, A. H. E. Müller and D. J. Pochan, *Macromolecules*, 2014, **47**, 1672-1683.
24 K. Hales, Z. Chen, K. L. Wooley and D. J. Pochan, *Nano Lett.*, 2008, **8**, 2023-2026.
25 W. Zhao, D. Chen, Y. Hu, G. M. Grason and T. P. Russell, *ACS Nano*, 2011, **5**, 486-492.
26 H. Schlaad, L. You, R. Sigel, B. Smarsly, M. Heydenreich, A. Mantion and A. Masic, *Chem. Commun.*, 2009, **45**, 1478-1480.
27 F. Liu and A. Eisenberg, *J. Am. Chem. Soc.*, 2003, **125**, 15059-15064.
28 L. Luo and A. Eisenberg, *J. Am. Chem. Soc.*, 2001, **123**, 1012-1013.
29 R. Stoenescu and W. Meier, *Chem. Commun*., 2002, **24**, 3016-3017
30 S. Schrage, R. Sigel and H. Schlaad, *Macromolecules*, 2003, **36**, 1417-1420.
31 Q. Liu, J. Chen and J. Du, *Biomacromolecules*, 2014, **15**, 3072-3082.
32 M. T. Roy, M. Gallardo and J. Estelrich, *Bioconjugate Chem.*, 1997, **8**, 941-945.
33 Y. Mai and A. Eisenberg, *Chem. Soc. Rev.*, 2012, **41**, 5969-5985.
34 N. J. Warren and S. P. Armes, *J. Am. Chem. Soc.*, 2014, **136**, 10174-10185.
35 B. Charleux, G. Delaittre, J. Rieger and F. D'Agosto, *Macromolecules*, 2012, **45**, 6753-6765.
36 J. Sun, C. Hong and C. Pan, *Polym. Chem.*, 2013, **4**, 873-881.
37 D. Zehm, L. P. D. Ratcliffe and S. P. Armes, *Macromolecules*, 2013, **46**, 128-139.
38 C. Gonzato, M. Semsarilar, E. R. Jones, F. Li, G. J. P. Krooshof, P. Wyman, O. O. Mykhaylyk, R. Tuinier and S. P. Armes, *J. Am. Chem. Soc.*, 2014, **136**, 11100-11106.

39 J. Rosselgong, A. Blanazs, P. Chambon, M. Williams, M. Semsarilar, J. Madsen, G. Battaglia and S. P. Armes, *ACS Macro Lett.*, 2012, **1**, 1041-1045.

40 W.-J. Zhang, C.-Y. Hong and C.-Y. Pan, *Macromolecules*, 2014, **47**, 1664-1671.

41 W. He, X. Sun, W. Wan and C.-Y. Pan, *Macromolecules*, 2011, **44**, 3358-3365.

42 X. Zhang, F. Boisson, O. Colombani, C. Chassenieux and B. Charleux, *Macromolecules*, 2014, **47**, 51-60.

43 Y. Pei and A. B. Lowe, *Polym. Chem.*, 2014, **5**, 2342-2351.

44 Y. Pei, N. C. Dharsana, J. A. van Hensbergen, R. P. Burford, P. J. Roth and A. B. Lowe, *Soft Matter*, 2014, **10**, 5787-5796.

45 W. Zhou, Q. Qu, W. Yu and Z. An, *ACS Macro Lett.*, 2014, **3**, 1220-1224.

46 R. Bleach, B. Karagoz, S. M. Prakash, T. P. Davis and C. Boyer, *ACS Macro Lett.*, 2014, **3**, 591-596.

47 S. Li, X. He, Q. Li, P. Shi and W. Zhang, *ACS Macro Lett.*, 2014, **3**, 916-921.

48 P. Shi, Q. Li, X. He, S. Li, P. Sun and W. Zhang, *Macromolecules*, 2014, **47**, 7442-7452.

49 X. He, Q. Li, P. Shi, Y. Cui, S. Li and W. Zhang, *Polym. Chem.*, 2014, **5**, 7090-7099.

50 Q. Li, X. He, Y. Cui, P. Shi, S. Li and W. Zhang, *Polym. Chem.*, 2015, **6**, 70-78.

51 J. T. Lai, D. Filla and R. Shea, *Macromolecules*, 2002, **35**, 6754-6756.

52 Y. He and T. P. Lodge, *Macromolecules*, 2008, **41**, 167-174.

53 C. Gao, S. Li, Q. Li, P. Shi, S. A. Shah and W. Zhang, *Polym. Chem.*, 2014, **5**, 6957-6966.

54 C. Gao, Q. Li, Y. Cui, F. Huo, S. Li, Y. Su and W. Zhang, *J. Polym. Sci., Part A: Polym. Chem.*, 2014, **52**, 2155-2165.

55 H. de Brouwer, M. A. J. Schellekens, B. Klumperman, M. J. Monteiro and A. L. German, *J. Polym. Sci., Part A: Polym. Chem.*, 2000, **38**, 3596-360.

56 A. Blanazs, J. Madsen, G. Battaglia, A. J. Ryan and S. P. Armes, *J. Am. Chem. Soc.*, 2011, **133**, 16581-16587.

57 N. J. Warren, O. O. Mykhaylyk, D. Mahmood, A. J. Ryan and S. P. Armes, *J. Am. Chem. Soc*., 2014, **136**, 1023-1033.

58 F. Huo, S. Li, Q. Li, Y. Qu and W. Zhang, *Macromolecules*, 2014, **47**, 2340-2349.

59 V. Pale, T. Nikkonen, J. Vapaavuori, M. Kostiainen, J. Kavakka, J. Selin, I. Tittonen and J. Helaja, *J. Mater. Chem. C.*, 2013, **1**, 2166-2173.

60 T. Koga, S. Kamiwatari and N. Higashi, *Langmuir*, 2013, **29**, 15477-15484.

61 L. Lei, J. Gohy, N. Willet, J. Zhang, S. Varshney and R. Jerome, *Macromolecules*, 2004, **37**, 1089-1094.

62 X. Li, J. Zuo, Y. Guo and X. Yuan, *Macromolecules*, 2004, **37**, 10042-10046.

For Table of Contents use only

Asymmetrical Vesicles: Convenient In Situ RAFT Synthesis and Controllable Structure Determination

Zefeng Song, Xin He, Chengqiang Gao, Habib Khan, Pengfei Shi, and Wangqing Zhang*

Key Laboratory of Functional Polymer Materials of the Ministry of Education, Collaborative Innovation Center of Chemical Science and Engineering (Tianjin), Institute of Polymer Chemistry, Nankai University, Tianjin 300071, China.

*To whom correspondence should be addressed. E-mail: (W. Zhang) wqzhang@nankai.edu.cn, Tel: +86-22-23509794, Fax: +86-22-23503510.

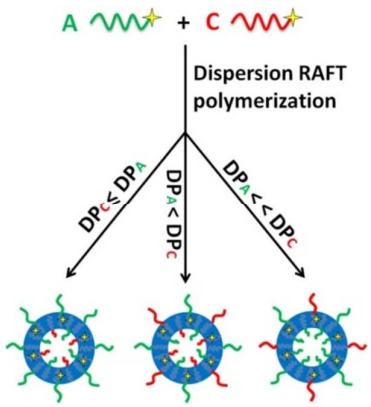

Asymmetrical vesicles of block copolymer were prepared, and the vesicle structure was found to be dependent on the polymerization degree of the solvophilic blocks.